

# Metal hydride formation in palladium and palladium rich intermetallic compounds studied by *in situ* neutron diffraction

H. Kohlmann <sup>a,\*</sup>, N. Kurtzemann <sup>b</sup>, T. C. Hansen <sup>c</sup>

<sup>a</sup> Institute of Inorganic Chemistry, Leipzig University, Leipzig, Germany

<sup>b</sup> Institute of Inorganic Solid State Chemistry, Saarland University, Saarbrücken, Germany

<sup>c</sup> Institut Laue-Langevin, Grenoble, France

\* correspondence author, holger.kohlmann@uni-leipzig.de, +49 341 97 36201

In order to investigate the hydrogenation of intermetallic compounds, a gas pressure cell for *in situ* neutron powder diffraction based on a sapphire crystal tube was constructed. By proper orientation of the single crystal Bragg peaks of the container material can be avoided, resulting in a very low diffraction background. Using a laser heating and gas pressure controller, the hydrogenation (deuteration) of palladium and palladium rich intermetallics was studied in real time up to 8 MPa gas pressure and 700 K. Crystal structure parameters of palladium deuterides could be obtained under various deuterium gas pressures, corresponding to compositional ranges of  $0.04 \leq x \leq 0.11$  for the  $\alpha$ -phase and  $0.52 \leq x \leq 0.72$  for the  $\beta$ -phase at 446 K. *In situ* neutron powder diffraction of the deuteration of a thallium lead palladium intermetallic  $Tl_{1-x}Pb_xPd_3$  shows two superstructures of the cubic closest packing (ccp) to transform independently into a  $AuCu_3$  type structure. This proves a direct reaction to the deuterium filled  $AuCu_3$  type structure instead of a reaction cascade involving different ccp superstructures and thus gives new insights into the reaction pathways of palladium rich intermetallic compounds

Key words:: *in situ* neutron diffraction, metal hydrides, hydrogen storage, hydrogenation, reaction pathways, palladium deuteride

## 1. Introduction

Research on compounds formed by intermetallic phases with gaseous hydrogen, metal hydrides, is often driven by their use as hydrogen storage media. Hydrogen can be generated from water by almost any primary energy including renewable sources, is therefore of unlimited availability and is considered a very interesting secondary energy source. Upon use it is environmentally friendly and liberates large amounts of energy according to the chemical reaction  $2 \text{H}_2 + \text{O}_2 \rightarrow 2 \text{H}_2\text{O} + 571.6 \text{ kJ/mol}$ . One of the key challenges for a hydrogen based energy economy (Winter, 2009) is the efficient and safe storage of large amounts of hydrogen. Solid compounds are being studied for this purpose, in which hydrogen is either stored by physisorption, typically at low temperatures, or by chemisorption, i. e. the formation of metal hydrides according to the reaction  $\text{M} + h/2 \text{H}_2 \rightarrow \text{MH}_h$  (Züttel, 2004; Graetz, 2009; Eberle *et al.*, 2009). Besides gravimetric and volumetric hydrogen density of the storage media, their cost, sensitivity to air, toxicity, and reversibility of the hydrogenation-dehydrogenation process are important issues in view of a potential use in hydrogen storage. Unfortunately, none of the current hydrogen storage materials fulfils all these requirements at the same time.

For the investigation of the process of hydrogen uptake of such storage materials and of the hydrogen liberation by dehydrogenation of the metal hydrides formed, *in situ* techniques allowing real time studies are very useful. This is particularly important for some new light-weight hydrogen storage materials such as metal boranates (also called borohydrides), alanates, amides, or imides, to name just a few, most of which lack reversibility in the hydrogenation-dehydrogenation reaction. Exploring reaction pathways including the discovery and characterization of intermediates may help to understand issues like reaction rates and reversibility. For the structural characterization the use of neutron diffraction has certain advantages over other diffraction methods in this case. Localizing light atoms such as hydrogen (deuterium), lithium, boron or nitrogen, which are important constituents of many storage materials is often easier due to more favourable diffraction cross sections as compared to XRD. The low absorption cross section for thermal neutrons of most materials is helpful for the construction of *in situ* equipment, since the penetration of bulky sample environment by neutrons is usually not an insurmountable problem. Further advantages are the possibility to distinguish between neighbouring elements in the periodic table of the elements, such as magnesium and aluminium or nitrogen and oxygen, and the accurate determination of thermal displacement

parameters, which yields important information in the vicinity of structural phase transitions of the decomposition of metal hydrides.

*In situ* neutron diffraction following the temperature (Wu *et al.*, 1995; Latroche *et al.*, 1998; Kohlmann and Yvon, 2000; Kohlmann *et al.*, 2001; Bogdanova, 2006; Filinchuk *et al.*, 2008; Kohlmann, 2009) and / or pressure dependence (Goncharenko *et al.*, 1992; Tellgren *et al.*, 2001; Kohlmann *et al.*, 2008) of structural parameters of metal hydrides are numerous and may give useful information on hydrogen storage materials. Real time *in situ* neutron diffraction experiments on hydrogenation reaction of intermetallic compounds, however, are rather scarce especially when high gas pressures are involved. This is due to the requirements for gas pressure cells, which may serve as sample holder in such hydrogenation experiments, such as pressure and temperature stability, chemical inertness toward hydrogen, little interference with the neutron beam and low diffraction background. Ideal materials for the fulfillment of the former conditions are cylindrical containers made of hydrogen resistant steel or other alloys, however, at the cost of parasitic reflections from the container material (Kuks *et al.*, 2005; Yartys *et al.*, 2010). Zero-scattering alloys made of zirconium and titanium cannot be used because of their strong hydrogen embrittlement. A very elegant solution to the problem of parasitic reflections from the container material was perfected for time of flight (TOF) spectroscopic measurements. A cylinder made from a zirconium-titanium zero-scattering alloy is protected from hydrogen embrittlement by an inner liner of Inconel 718 alloy, whose contribution to the diffraction pattern is properly masked out for the 90° detector bank (Gray *et al.*, 2007). This technique requires a careful attenuation correction and is restricted to TOF experiments. For inelastic neutron scattering the use of sapphire single crystals as sample holders was proven useful for avoiding Bragg peaks of the container material (Rondinone *et al.*, 2003). This concept was later adapted to elastic neutron scattering in *in situ* neutron powder diffraction by using a 6 mm wide borehole in a 10 cm long sapphire single crystal as sample chamber, attached to a hydrogen (deuterium) gas pressure control and a laser heating system (Kohlmann *et al.*, 2009a). By proper orientation of the sapphire sample holder, a complete avoidance of its Bragg peaks by the detector of the powder diffractometer could be achieved, thus allowing high quality neutron powder diffraction data collected in real time under *in situ* conditions. In this contribution we describe the use of this piece of sample environment to the study of the reaction of palladium and palladium rich intermetallic phases with hydrogen (deuterium).

## 2. Experimental details

### 2.1 Isotopes of hydrogen and nomenclature

Experiments have been carried out using deuterium gas with an isotopic purity of 99.8% for neutron powder diffraction. Only when referring to experiments with this method a clear distinction will be made between hydrogen and deuterium, hydride and deuteride and so on, while for general discussions the terms *hydrogen*, *hydride* and *hydrogenation* are used in a generic way for the natural isotopic mixture as well as for deuterium. This is justified, because isotope effects are generally small enough to not affect the conclusions drawn here. More details on isotope effects of hydrogen in neutron diffraction can be found in (Weller *et al.*, 2008; Ting *et al.*, 2010).

### 2.2 Synthesis and specimen preparation

In order to get a completely hydrogen free starting material and to activate it, palladium powder (< 60 micron, 99.9+%, ChemPur) was degassed in a dynamic vacuum of 20 mPa at 500 °C for 1 h. After cooling to room temperature it was kept in an argon atmosphere. Synthesis of all other starting materials is described elsewhere (Kohlmann *et al.*, 2010; Kurtzemann and Kohlmann, 2010). All materials were handled under inert gas atmosphere in an argon-filled glove box. For sample preparation they were ground in an agate mortar before filling into the gas pressure cell, in order to increase the surface area and thus the reactivity and to ensure a good crystallite statistics in the diffraction experiment.

### 2.3 *In situ* neutron powder diffraction (NPD)

Neutron powder diffraction data were taken *in situ* under various deuterium (isotopic purity 99.8%) gas pressures up to 10 MPa at the Institute Laue-Langevin in Grenoble, France, on the high intensity powder diffractometer D20 (Hansen *et al.*, 2008) in high resolution mode (average resolution  $\Delta d/d = 3 \cdot 10^{-3}$ ) in the range  $3^\circ \leq 2\theta \leq 150^\circ$  (0.1 ° step width in  $2\theta$ ). Depending on reflection intensities, signal to background ratio and the speed of the reaction, time resolution between 2 and 4 min per pattern were chosen. Deuterium was used in order to avoid the strong incoherent scattering of the  $^1\text{H}$  (protium) isotope of hydrogen. For a detailed discussion of isotope effects in metal hydrides and hydrogenous materials in general and with regard to neutron diffraction see references (Weller *et al.*, 2008; Ting *et al.*, 2010). The sample was placed inside a single crystal sapphire based gas pressure cell especially designed for *in situ* neutron powder diffraction. The deuterium gas pressure was varied by a gas pressure controller during

the measurements and the sample was heated using a contactless laser heating system. Temperature was measured by a pyrometer that was calibrated against the lattice parameter of palladium refined from neutron diffraction data using the same sapphire gas pressure cell. For a more detailed description of the experimental setup see (Kohlmann *et al.*, 2009a; Widenmeyer *et al.*, 2013). The neutron wavelengths used were determined from measurements on a NIST 640b silicon standard and kept fixed during subsequent refinements. Rietveld refinements were carried out with the program FullProf (Rodriguez-Carvajal, 2011) and pseudo-Voigt as profile function.

### 3. Results and Discussion

#### 3.1 The deuteration of palladium

For testing the sapphire single crystal gas pressure cell palladium is an ideal test case, because the Pd-H(D) phase diagram is very well known (Flanagan and Oates, 1991). At room temperature an  $\alpha$ -phase PdH<sub>x</sub> with a narrow phase width of about  $0 \leq x \leq 0.02$  and a  $\beta$ -phase with a much wider range of  $0.6 \leq x \leq 1.0$  exist (Fig. 1), both with a disordered arrangement of hydrogen (deuterium) in octahedral voids of a cubic closest packing of palladium atoms. Thus, all three phases, palladium,  $\alpha$ -palladium hydride (deuteride) and  $\beta$ -palladium hydride (deuteride) exhibit the same topology of the palladium substructure, i. e. a cubic closest packing, and differ only by their respective hydrogen (deuterium) occupation. At a critical temperature of 563 K and a critical pressure of 1.9 MPa for the hydride and 556 K and 3.9 MPa for the deuteride and a hydrogen content  $x = 0.257$  for both the miscibility gap vanishes and one homogeneous phase with  $0 \leq x \leq 1.0$  exists (Fig. 1) (Flanagan and Oates, 1991). Using the sapphire gas pressure cell, the deuteration of palladium powder has been followed at  $T = 446(4)$  K with a time resolution of two minutes *in situ* by neutron powder diffraction (Fig. 2). The pressure was increased step-wise, as indicated in Figs. 2 and 3.

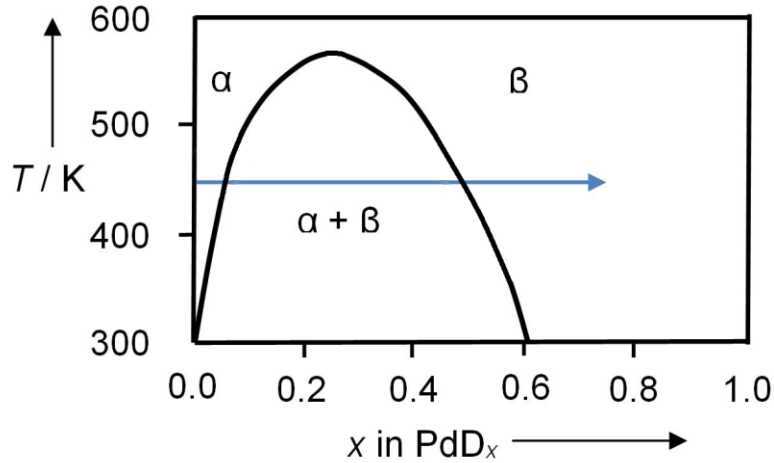


Fig. 1: Phase diagram of the palladium-deuterium system adapted from (Flanagan and Oates, 1991); arrow indicates the pathway of the *in situ* diffraction experiment shown in Fig. 2.

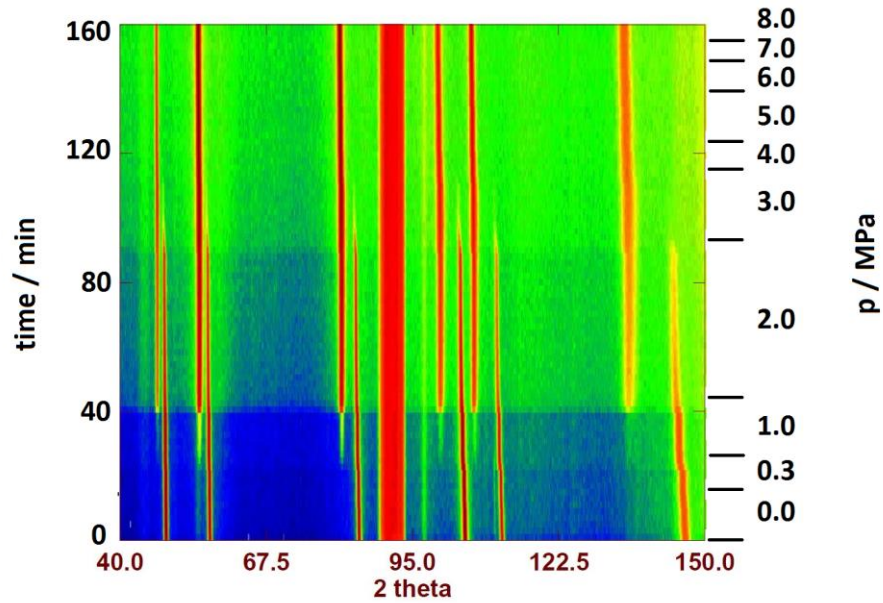


Fig. 2: Neutron powder diffraction data of palladium deuteride at  $T = 446(4)$  K taken *in situ* on D20 (ILL, Grenoble) at  $\lambda = 186.71(1)$  pm in a single crystal sapphire gas pressure cell with a time resolution of 2 min, intensities on a logarithmic scale in false color (lowest intensity blue, highest intensity red. The range  $87^\circ \leq 2\theta \leq 95^\circ$  (red bar in online edition, black in print edition) was excluded from refinements due to scattering from the sapphire single crystal.

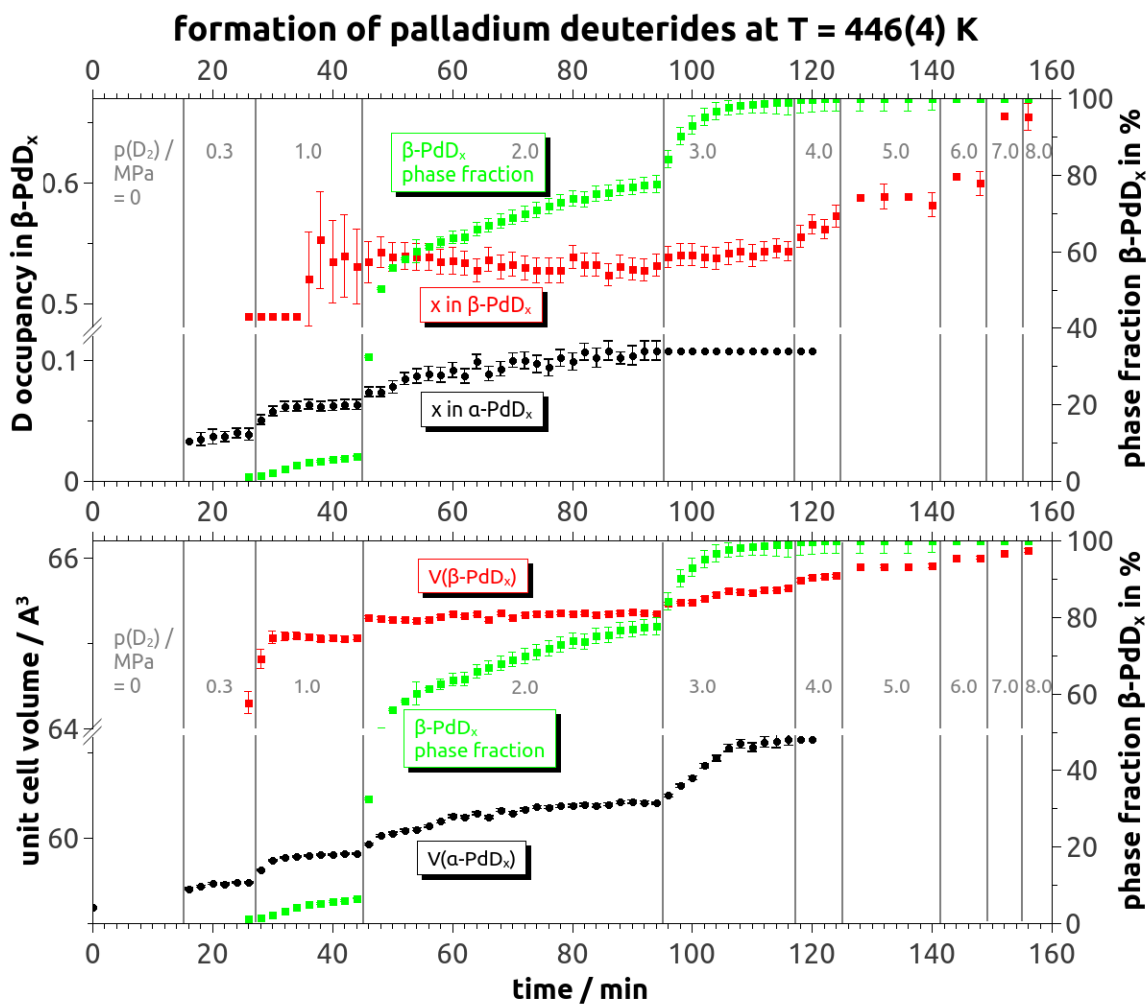


Fig. 3: Results of Rietveld refinements of the crystal structures of  $\alpha$ - and  $\beta$ -PdD<sub>x</sub> as a function of time based on *in situ* neutron powder diffraction data represented in Fig. 2. Deuterium pressure is indicated in inserts. Error bars represent one estimated standard uncertainty.

Due to the rather long wavelength the accessible Q range is rather small and only six reflections, i. e. (111), (200), (220), (311), (222), and (400) of the  $\alpha$ - and  $\beta$ -phase deuteride could be obtained (Fig. 2). In the two-dimensional representation of Fig. 2 the reflections appear as lines running up along the time axis, shifting due to deuterium uptake and / or temperature changes and fading away, when the phase disappears. In the first few runs a slight shifting of reflections (seen only at higher diffraction angles) indicates temperature still increasing to its final value of 446(4) K. After 15 min, deuterium is introduced at a pressure of 0.3 MPa, which immediately results in formation of the  $\alpha$ -phase. The deuterium uptake can be seen by a slight shift to lower diffraction angles, i. e. higher *d* values (Figs. 2 and 3). Only a few minutes later, formation of the  $\beta$ -phase starts as seen by the appearance of new diffraction peaks (Fig. 2). For a period of 96

minutes both  $\alpha$ - and  $\beta$ -phase deuteride coexist. The deuterium content of the  $\alpha$ -phase deuteride  $\text{PdD}_x$  start at  $x = 0.038(4)$  at a deuterium pressure of 0.3 MPa and reaches a maximum of  $x = 0.108(8)$  at 2.0 MPa. At pressures up to 1.0 MPa the formation of the  $\beta$ -phase is slow and less than 10% of the  $\alpha$ -phase was converted after 45 minutes of the experiment. Upon increasing the deuterium gas pressure to 2.0 MPa, however, 50% of the  $\alpha$ -phase was converted into the  $\beta$ -phase within only four minutes. The reaction rate then slows down and the reaction is complete after two hours (Fig. 3) with no trace of  $\alpha$ - $\text{PdD}_x$  reflections left. The deuterium content of the  $\beta$ -phase continues to grow with increasing pressure to a maximum corresponding to a composition of  $\beta$ - $\text{PdD}_{0.72(3)}$  at  $T = 446(4)$  K and 8.0 MPa deuterium pressure. Incorporation of tetrahedral voids was not observed in the course of this *in situ* study.

After each pressure increase, the unit cell volume of the  $\alpha$ -phase increases slowly, while that of the  $\beta$ -phase does so very quickly (Fig. 3). This is probably due to the well-known fact that diffusion of hydrogen in the former is slower than in the latter (Storms, 1998). Accordingly, deuterium occupation increases slowly with time in the  $\alpha$ -phase, while in the  $\beta$ -phase it increases almost instantly stepwise at pressure rise and then stays constant (Fig. 3). This further suggests that deuterium diffusion is the time-limiting step, at least for the formation of the  $\alpha$ -phase deuteride  $\text{PdD}_x$ . It should be emphasized at this point, that both  $\alpha$ - and the  $\beta$ -phase show the same cubic closest packing of palladium and differ only by the extent of occupation of octahedral voids by deuterium.

In order to handle low phase fractions and large correlation of the thermal displacement (Debye-Waller factor  $B_{\text{iso}}$ ) and occupation parameter of deuterium the following Rietveld refinement strategy was followed. (i)  $\alpha$ - $\text{PdD}_x$ : For a deuterium content of  $x < 0.1$ ,  $B_{\text{iso}}(\text{D})$  was fixed at  $4.5 \text{ \AA}^2$ . This is a reasonable value, since refinements in the  $\beta$ -phase with larger unit cell volumes gives values around  $5.0 \text{ \AA}^2$  at this temperature. For phase contents below 15%,  $B_{\text{iso}}(\text{Pd})$  and the occupation parameter of the deuterium atoms are fixed to the values refined in the former runs. For the last two data sets with content of the  $\alpha$ -phase, the phase content drops below 1% and the lattice parameter had to be fixed to the value refined in the run just before that one. (ii)  $\beta$ - $\text{PdD}_x$ : For phase fraction below 10%  $B_{\text{iso}}$  values were fixed to  $1.0 \text{ \AA}^2$  for palladium and to  $5.0 \text{ \AA}^2$  for deuterium atoms, which are values typically found in later refinements with larger phase fractions. For phase contents below 5% the deuterium occupation was fixed to  $x = 0.49$  in accordance with the phase diagram and later refinements.



The *in situ* neutron powder diffraction data collected on the deuteration of palladium and their results by Rietveld refinement prove the potential of the sapphire gas pressure cell for real time studies of hydrogenation (deuteration) reactions. Some general features of such experiments are also clearly exposed. Fig. 2 shows how the diffraction background between the Bragg peaks increases with time, i. e. with increasing deuterium gas pressure. This is due to the incoherent scattering of deuterium incorporated in large amounts in the  $\beta$ -phase palladium deuteride as well as the increased amount of deuterium gas in the sapphire cell. The logarithmic scale in Fig. 2 enhances such small contributions to the diffraction patterns elucidating this effect nicely. The evolution of position and intensity of Bragg peaks with time (Fig. 2) shows some distinct kinks, especially after pressure increase where drastic changes in deuterium content and lattice parameters are observed. This shows clearly that a time resolution of two minutes is not sufficient for this reaction. While the accuracy of structural parameters seems good for an *in situ* neutron powder diffraction study that of deuterium occupation parameters could be easily enhanced by using a shorter wavelength.

### 3.2 Hydrogen induced rearrangements in palladium rich intermetallics $MPd_3$ ( $M = Mg, In, Tl, Tl_{1-x}Pb_x$ )

In  $AuCu_3$  type structures of intermetallics compounds hydrogen often occupies octahedral interstices made up of six palladium atoms,  $[Pd_6]$  voids (Schwarz *et al.*, 1991; Önnnerud *et al.*, 1997; Yamaguchi *et al.*, 1997; Tellgren *et al.*, 2001; Vennström *et al.*, 2004; Kohlmann *et al.*, 2009b; Kurtzemann and Kohlmann, 2010; Kohlmann *et al.*, 2010). Some of these hydrides form by hydrogen induced rearrangement from other superstructures of the cubic closest packing (ccp), e. g. from compounds  $MPd_3$  ( $M = Mg, In, Tl, Tl_{1-x}Pb_x$ ) in the structure types of  $TiAl_3$ ,  $ZrAl_3$  or  $PbTl_2Pd_9$ . These structure types differ from the one of  $AuCu_3$  by the introduction of antiphase domains at different concentrations. The hydrogenation reactions show some very interesting and unusual features: (i) certain types of ccp superstructures are a necessary precondition (Kohlmann and Ritter, 2009), (ii) mild reaction conditions, (iii) small activation energy (Kunkel *et al.*, 2011).

Based on these observations a reaction mechanism of the hydrogen induced rearrangements in such palladium rich intermetallics  $MPd_3$  ( $M = Mg, In, Tl, Tl_{1-x}Pb_x$ ) was proposed. The ccp superstructures first take up hydrogen, which occupies  $[Pd_6]$  and to a lesser

extent  $[MPd_5]$  voids. Increasing temperature enhances diffusion in the solid and a crystallographic shear operation  $\frac{1}{2}$   $[110]$  of  $MPd_3$  slabs within the ccp superstructures occurs. This reduces the amount of antiphase domains, which ultimately leads to the cubic  $AuCu_3$  type structure for the metal atoms with hydrogen in octahedral  $[Pd_6]$  interstices only. The activation barrier for this type of gliding operation was calculated to be relatively low (Kunkel *et al.*, 2011). Data for  $M = Mg, In, Tl$  were presented earlier and confirm the proposed mechanism (Kohlmann *et al.*, 2009b; Kurtzemann and Kohlmann, 2010; Kohlmann *et al.*, 2010). It could now also be shown to work in a thallium rich compound  $Tl_{1-x}Pb_xPd_3$ , in which three modifications coexist:  $AuCu_3$ ,  $ZrAl_3$  and  $PbTl_2Pd_9$  type structures. Fig. 4 shows the evolution of Bragg peaks during an *in situ* neutron powder diffraction experiment in a small section of the powder pattern during a total reaction time of 18.5 h. As can be clearly seen, the (220) reflection of the deuteride with the cubic  $AuCu_3$  type structure for the metal atoms with deuterium in octahedral  $[Pd_6]$  interstices develops from the corresponding tetragonally split reflections of the  $ZrAl_3$  and  $PbTl_2Pd_9$  type modifications of the starting material. The final product is the deuteride of  $Tl_{1-x}Pb_xPd_3$  with a  $AuCu_3$  type arrangement for the metal atoms and deuterium surrounded by six palladium neighbours. Both modifications of the starting material, i. e. the  $ZrAl_3$  and  $PbTl_2Pd_9$  type structures vanish at approximately the same rate as the phase content  $AuCu_3$  type product grows (Fig. 4), instead of transforming into each other first. This sheds new light on these transitions because up to now only one ccp superstructure at a time could be studied *in situ* and the proposed reaction pathway (Kohlmann *et al.*, 2009b) could not distinguish between two scenarios: a direct transformation to the  $AuCu_3$  type on one hand and a cascade like reaction from  $TiAl_3$  to  $ZrAl_3$  and further to the  $PbTl_2Pd_9$  type modifications on the other hand. In the light of the present investigation, the latter possibility does not seem to be realized. It should be emphasized that these rearrangements in the intermetallic structure are caused solely by the incorporation of the hydrogen (deuterium) atoms. For a complete understanding of the transformation pathways neutron diffraction plays an important role due to its power in locating light elements such as hydrogen (deuterium) as compared to X-ray diffraction.

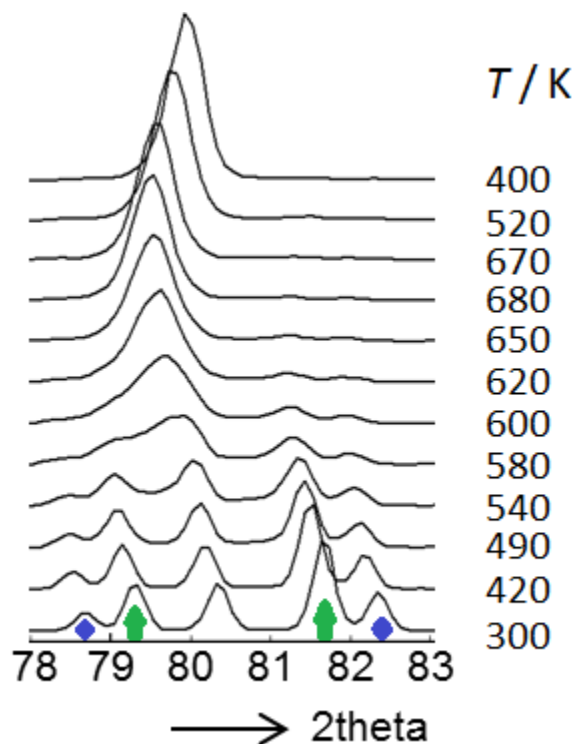


Fig. 4: Evolution of the (220) reflection of the cubic deuteride of a thallium rich compound  $Tl_{1-x}Pb_xPd_3$  in an *in situ* neutron powder diffraction experiment at  $p(D_2) = 20$  bar at various temperatures taken on D20 (ILL, Grenoble) at  $\lambda = 186.707(2)$  pm in a single crystal sapphire gas pressure cell; bottom: starting material with  $AuCu_3$  type (middle reflection),  $PbTl_2Pd_9$  (second and fourth reflection, indicated by green arrows on the bottom pattern) and  $ZrAl_3$  type (outer reflections, indicated by blue squares on the bottom pattern).

#### 4. Conclusion

A sapphire single crystal based gas pressure cell for *in situ* neutron powder diffraction was developed. By proper orientation of the single crystal its contribution to the diffraction pattern is negligible, which is an advantage over many other gas pressure cells. For the study of reactions of metals and intermetallic compounds it can be subjected to hydrogen gas pressures up to 160 bar. Heating is achieved by a two-sided laser system, in order to avoid interference with the diffraction experiment. This sample environment was setup at the neutron powder diffractometer D20 at the Institut Laue-Langevin in Grenoble, France. With a time resolution in the order of minutes high quality diffraction data can be collected, which allow for a detailed analysis of structural parameters by the Rietveld refinement technique. Examples presented are the hydrogenation of palladium and of palladium containing intermetallic phases. For palladium a detailed picture of the formation of  $\alpha$ - and  $\beta$ -palladium deuteride was observed, in agreement with the phase diagram, however, yielding new data not accessible before. In 80 Rietveld refinements structural parameters of such phases could be obtained under various deuterium gas

pressures, thus representing different compositions in the range  $0.04 \leq x \leq 0.11$  for the  $\alpha$ -phase and  $0.52 \leq x \leq 0.72$  for the  $\beta$ -phase. This demonstrates that this method allows collecting high quality neutron diffraction data and thus refined structural parameters under various temperature-pressure conditions *in situ* in a very short time. New insights could also be gained for the deuteration of palladium rich intermetallic phases. In a thallium lead palladium intermetallic two ccp superstructures transform independently into a  $\text{AuCu}_3$  type structure with deuterium occupying octahedral voids. This helps distinguishing between different possible reaction pathways. In this case it proves a direct reaction to the deuterium filled  $\text{AuCu}_3$  type structure instead of a reaction cascade involving different ccp superstructures.

- Bogdanova, A. N. (2006). "Neutron Diffraction Study of Phase Transitions in Highly Concentrated Hydrogen Solid Solutions  $\text{ZrV}_2\text{D}_x$  ( $4 < x < 5$ )," *Phys. Solid State* **48**, 1351-1355.
- Eberle, U., Felderhoff, M. and Schüth, F. (2009). "Chemische und physikalische Lösungen für die Speicherung von Wasserstoff," *Angew. Chem.* **121**, 6732-6757.
- Filinchuk, Y., Chernyshov, D. and Dmitriev, V. (2008). "Light metal borohydrides: crystal structures and beyond," *Z. Kristallogr.* **223**, 649-659.
- Flanagan, T. B. and Oates, W. A. (1991). "The palladium-hydrogen system," *Annu. Rev. Mater. Sci.* **21**, 269-304.
- Goncharenko, I. N. , Glazkov, V. P., Irodova, A. V., Lavrova, O. A. and Somenkov, V. A. (1992). "Compressibility of dihydrides of transition metals," *J. Alloys Compd.* **179**, 253-257.
- Graetz, J. (2009). "New approaches to hydrogen storage," *Chem. Soc. Rev.* **38**, 73-82.
- Gray, E. MacA., Smith, R. I. and Pitt, M. P. (2007). "Time-of-flight neutron powder diffraction with a thick-walled sample cell," *J. Appl. Crystallogr.* **40**, 399-408.
- Hansen, T. C., Henry, P. F., Fischer, H. E., Torresgrossa, J. and Convert, P. (2008). "The D20 instrument at the ILL: a versatile high-intensity two-axis neutron diffractometer," *Meas. Sci. Technol.* **19**, 034001.
- Kohlmann, H. (2009). "Structural relationships in complex hydrides of the late transition metals," *Z. Kristallogr.* **224**, 454-460.
- Kohlmann, H., Fauth, F., Fischer, P. Skripov, A. V. and Yvon, K. (2001). "Low-temperature deuterium ordering in the cubic Laves phase derivative  $\alpha\text{-ZrCr}_2\text{D}_{0.66}$ ," *J. Alloys Compd.* **327**, L4-L9.

- Kohlmann, H., Kurtzemann, N., Wehrich, R. and Hansen, T. (2009a). "In situ neutron powder diffraction on intermediate hydrides of  $\text{MgPd}_3$  in a novel sapphire gas pressure cell," *Z. Anorg. Allg. Chem.* **635**, 2399-2405.
- Kohlmann H., Müller, F., Stöwe, K., Zalga, A. and Beck, H. P. (2009b). "Hydride formation in the intermetallic compounds  $\text{CePd}_3$  and  $\text{CeRh}_3$ ," *Z. Anorg. Allg. Chem.* **635**, 1407-1411.
- Kohlmann, H. and Ritter, C. (2009). "Reaction Pathways in the Formation of Intermetallic  $\text{InPd}_3$  Polymorphs," *Z. Anorg. Allg. Chem.* **635**, 1573-1579.
- Kohlmann, H., Skripov, A. V., Solonin, A. V. and Udovic, T. J. (2010). "The anti-perovskite type hydride  $\text{InPd}_3\text{H}_{0.89}$ ," *J. Solid State Chem.* **183**, 2461-2465.
- Kohlmann, H. and Yvon, K. (2000). "Revision of the low-temperature structures of rhombohedral  $\text{ZrCr}_2\text{D}_x$  ( $x \sim 3.8$ ), and monoclinic  $\text{ZrV}_2\text{D}_x$  ( $1.1 < x < 2.3$ ) and  $\text{HfV}_2\text{D}_x$  ( $x \sim 1.9$ )," *J. Alloys Compd.* **309**, 123-126.
- Kohlmann, H., Zhao, Y., Nicol, M. F. and McClure, J. (2008). "The crystal structure of  $\alpha\text{-MgD}_2$  under high pressure by neutron powder diffraction," *Z. Kristallogr.* **223**, 706-710.
- Kuhs, W. F., Hensel, E. and Bartels, H. (2005). "Gas pressure cells for elastic and inelastic neutron scattering," *J. Phys.: Condens. Matter* **17**, S3009-S3015.
- Kunkel, N., Sander, J., Louis, N., Pang, Y., Dejon, L. M., Wagener, F., Zang, Y. N., Sayede, A., Bauer, M., Springborg, M. and Kohlmann, H. (2011). "Theoretical investigation of the hydrogenation induced atomic rearrangements in palladium rich intermetallic compounds  $\text{MPd}_3$  ( $M = \text{Mg, In, Tl}$ )," *Eur. Phys. J. B* **82**, 1-6.
- Kurtzemann, N., Kohlmann, H. (2010). "Crystal Structure and Formation of  $\text{TlPd}_3$  and its new Hydride  $\text{TlPd}_3\text{H}$ ," *Z. Anorg. Allg. Chem.* **636**, 1032-1037.
- Latroche, M., Paul-Boncour, V., Percheron-Guégan, A. and Bourée-Vignon, F. (1998). "Temperature dependence study of  $\text{YMn}_2\text{D}_{4.5}$  by means of neutron powder diffraction," *J. Alloys Compd.* **274**, 59-64.
- Önnerud, P., Andersson, Y., Tellgren, R., Norblad, P., Bourée, F. and André, G. (1997). "The Crystal and Magnetic Structures of Ordered Cubic  $\text{Pd}_3\text{MnD}_{0.7}$ ," *Solid State Commun.* **101**, 433-437.
- Rodriguez-Carvajal, J. (2011). FULLPROF 2.k, version 5.2, Jul2011-ILL (Computer Software) JRC, Grenoble.
- Rondinone, A. J. Jones, C. Y., Marshall, S. L., Chakoumakos, B. C., Rawn, C. J. and Lara-Curizo, E. (2003). "A Single-Crystal Sapphire Cell for in situ Neutron Diffraction Study of Gas-Hydrate," *Can. J. Phys.* **81**, 381-385.
- Schwarz, D. S., Yelon, W. B., Berliner, R. R., Lederich, R. J. and Sastry, S. M. L. (1991). "A novel hydride phase in hydrogen charged  $\text{Ti}_3\text{Al}$ ," *Acta Metall. Mater.* **39**, 2799-2803

- Storms, E. (1998). "Formation of  $\beta$ -PdD containing high deuterium concentration using electrolysis of heavy-water," J. Alloys Compd. **268**, 89-99.
- Tellgren, R., Andersson, Y., Goncharenko, I., André, G., Bourée, F. and Mirebeau, I. (2001). "High-Pressure Neutron Diffraction Studies of the Magnetic Structures of Cubic Pd<sub>3</sub>MnD<sub>0.7</sub>," J. Solid State Chem. **161**, 93-96.
- Ting, V. P., Henry, P. F., Kohlmann, H., Wilson, C. C. and Weller, M. T. (2010). "Structural isotope effects in metal hydrides and deuterides," Phys. Chem. Chem. Phys. **12**, 2083-2088.
- Vennström, M., Grechnev, A., Eriksson, O. and Andersson, Y. (2004). "Phase relations in the Ti<sub>3</sub>Sn-D system," J. Alloys Compd. **364**, 127-131.
- Weller, M. T., Henry, P. F., Ting, V. P. and Wilson, C. C. (2008). "Crystallography of hydrogen-containing compounds: realizing the potential of neutron powder diffraction," Chem. Commun. (Cambridge, U. K.), 2973-2989.
- Widenmeyer, M., Niewa, R., Hansen, T. C., and Kohlmann, H. (2013). "In situ Neutron Diffraction as a Probe on Formation and Decomposition of Nitrides and Hydrides: A Case Study," Z. Anorg. Allg. Chem. **639**, 285-295.
- Winter, C. J. (2009). "Hydrogen energy - Abundant, efficient, clean: A debate over the energy-system-of-change," Int. J. Hydrogen Energy **34**, S1-S52.
- Wu, E., Kennedy, S. J., Kisi, E. H., Mac A. Gray, E. and Kennedy, B. J. (1995). "Neutron powder diffraction study of deuterium ordering in  $\beta$  phase Pd-D at low temperatures," J. Alloys Compd. **231**, 108-114.
- Yamaguchi, S., Ohashi, M., Kajitani, T., Aoki, K., and Ikeda, S. (1997). "Distribution of hydrogen atoms in YPd<sub>3</sub>H<sub>x</sub> studied by neutron diffraction and inelastic neutron scattering," J. Alloys Compd. **253-254**, 308-312.
- Yartys, V. A., Denys, R. V., Maehlen, J. P., Webb, C. J., Gray, E. MacA., Blach, T., Poletaev, A. A., Solberg, J. K. and Isnard, O. (2010). "Nanostructured Metal Hydrides for Hydrogen Storage Studied by In Situ Synchrotron and Neutron Diffraction," Mater. Res. Soc. Symp. Proc. **1262**, W04-01.
- Züttel, A. (2004). "Hydrogen storage methods," Naturwissenschaften **91**, 157-172.